Supplementary information – Figures

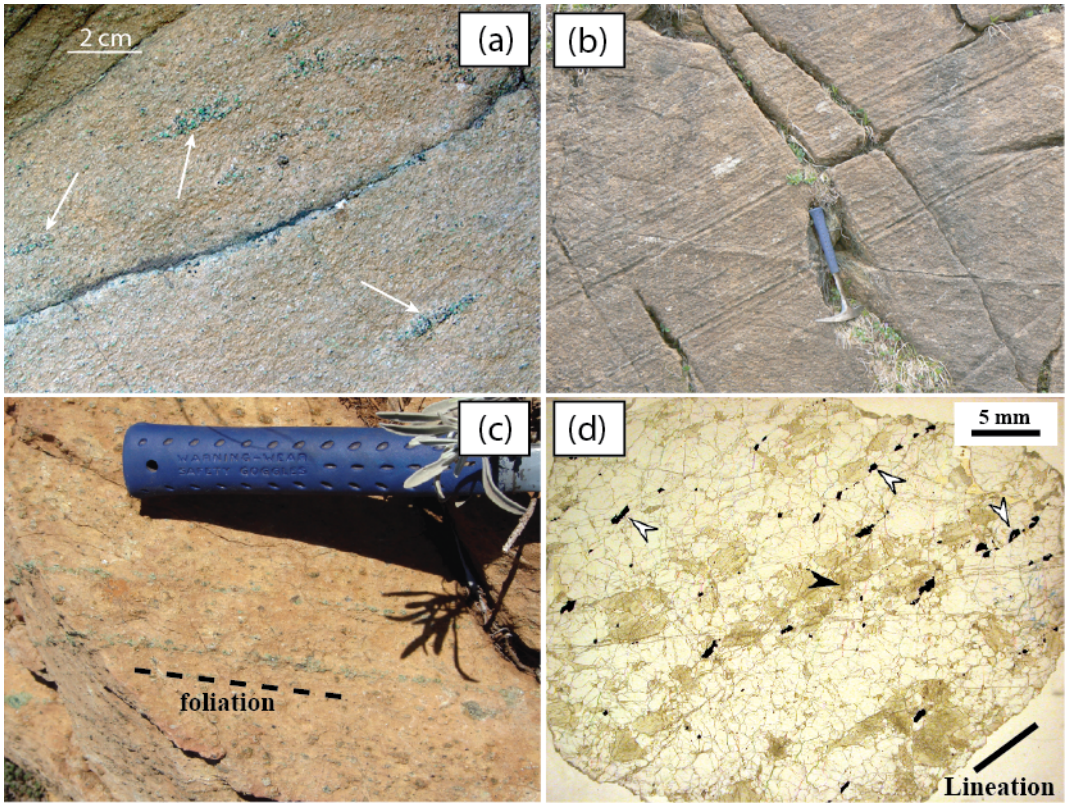

Figure DR1. (a) Foliation-parallel websteritic lenses as a result of melt percolation in deforming harzburgite. (b) Pervasive websteritic layering in refertilized lherzolite resulting from deformation-assisted melt segregation. (a) and (b) are outcrop from the Lherz massif, France, and have been reported by Le Roux et al. (2008). (c) Foliation-parallel clinopyroxene-rich bands resulting from refertilization processes coeval with high-temperature deformation in harzburgite from the spinel-tectonite domain of the Ronda peridotite massif, Spain (see Soustelle et al., 2009). (d) Orthopyroxene-rich band (black arrow) parallel to the lineation underlined by the spinel trail (white arrows) in peridotite xenoliths from Avacha volcano, Kamchatka. The parallelism is due to reactive percolation of Si-fluid crystallizing orthopyroxene at the expense of the olivine synchronous with a high-temperature deformation event (Soustelle et al., 2010).

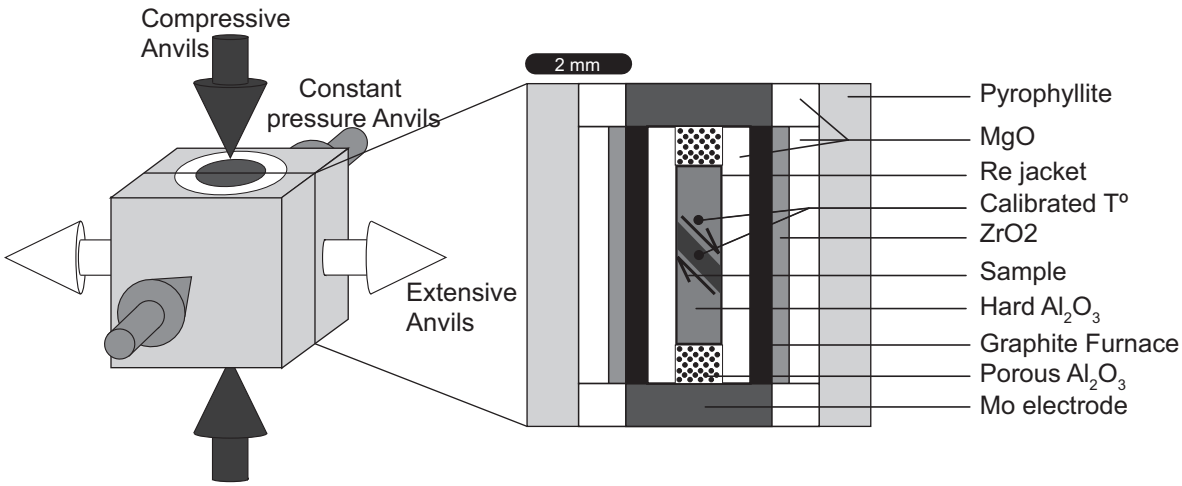

Figure DR2. Schematic diagram of sample assemblies and deformation geometry.

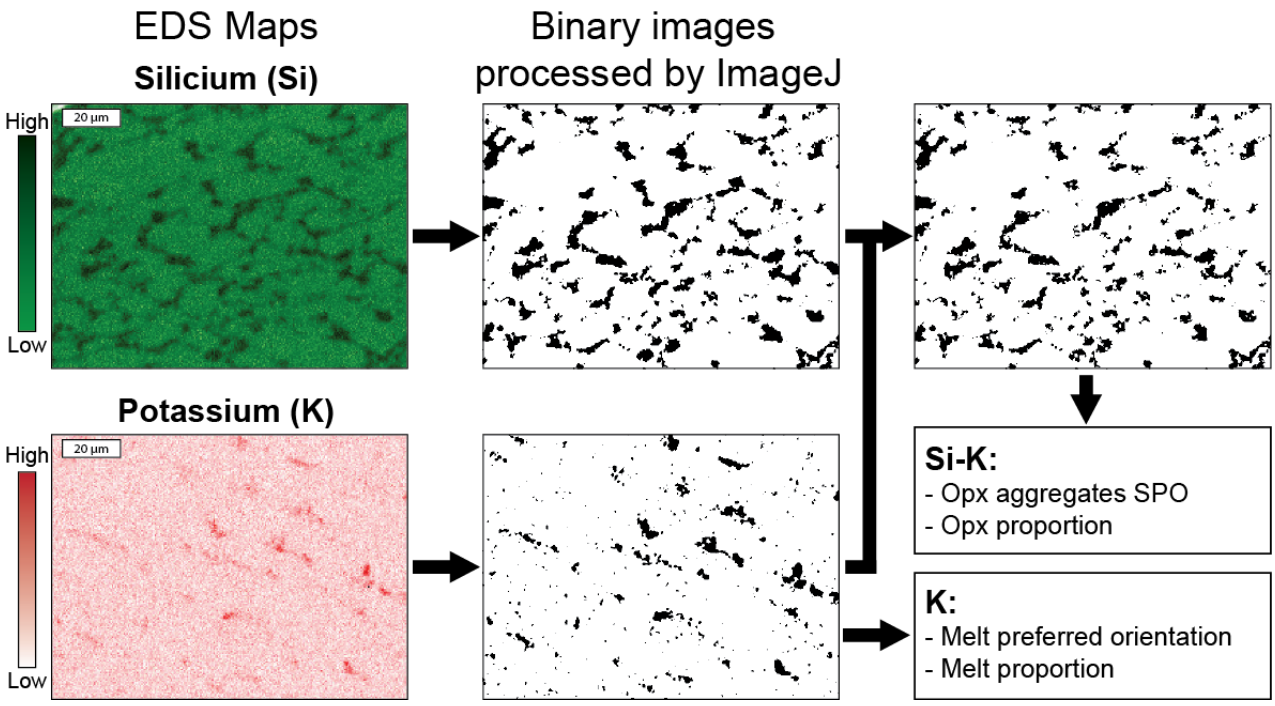

Figure DR3. Binary processed images from Si and K EDS maps. Binary images from K EDS map are used to calculate the melt preferred orientation (example of data are shown in Table 3 of the supplementary information) and the melt proportion (total of the black pixels area divided by the total area). As Si concentration is high in melt and pyroxene, the binary image resulting from the subtraction of the Si EDS map by the K EDS map is used to calculate orthopyroxene (opx) aggregate SPO and opx proportion.

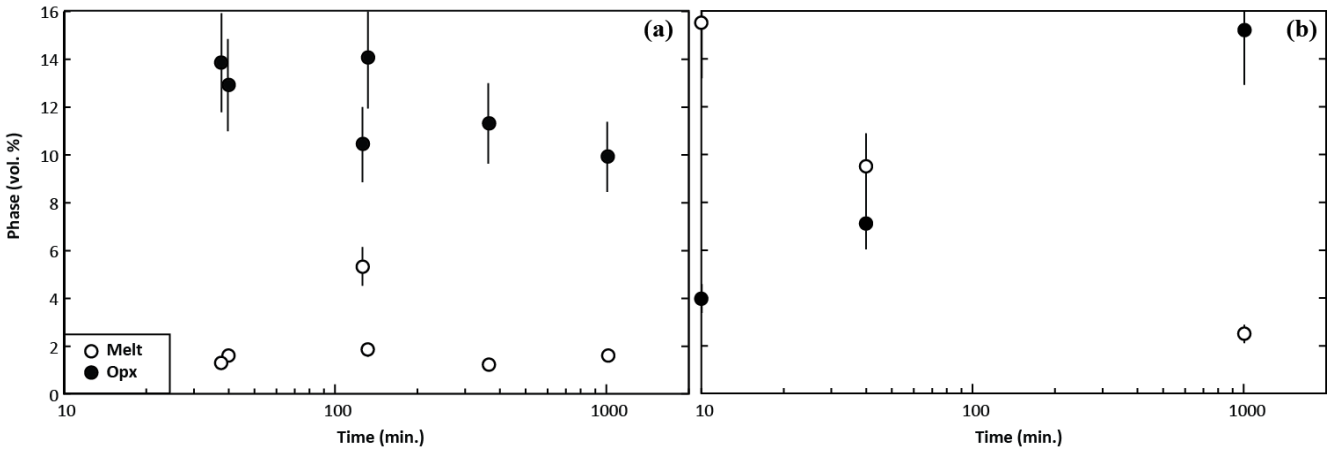

Figure DR4. Orthopyroxene (opx) and melt proportion as a function of time for deformation (a) and static (b) experiments.

Supplementary information - Tables

Table DR1. Microprobe analyses of starting olivine and melt.

	San Carlos olivine		Melt M7-1	
	Average(21)[a] (wt. %)	*Stdev*[b]	Average(16)[a] (wt. %)	*Stdev*[b]
SiO2	40.303	*0.218*	74.024	*0.364*
Na2O	0.012	*0.014*	6.436	*0.143*
K2O	0.007	*0.011*	5.516	*0.088*
CaO	0.069	*0.012*	2.297	*0.039*
FeO	9.403	*0.545*	3.448	*0.063*
MgO	49.243	*0.484*	0.854	*0.026*
Al2O3	0.018	*0.014*	4.208	*0.062*
TiO2	0.009	*0.014*	1.228	*0.046*
Mg#	0.903	*0.006*	-	-
Total	99.064		98.010	

[a] Number of analyses
[b] Stdev = standard deviation

Table DR2. Example* of data extracted from binary images used for MPO and orthopyroxene aggregate SPO calculation

Patch Number	Area (pixels)	Average ellipsoid major axis length (pixels)	Average ellipsoid minor axis length (pixels)	Angle of the major axis (º)
1	548	29.556	23.607	91.686
2	487	35.5	17.467	27.957
3	389	33.168	14.933	49.887
4	353	32.799	13.703	3.878
5	308	40.647	9.648	16.446
6	282	26.911	13.342	48.082
7	273	27.722	12.539	170.2
8	253	21.887	14.718	78.38
9	195	21.704	11.44	55.217
10	194	24.882	9.927	37.211
11	193	26.41	9.305	40.464
12	192	22.109	11.057	38.057
13	178	19.178	11.818	44.771
14	156	17.55	11.318	25.204
15	155	16.682	11.83	76.55
16	127	17.108	9.452	34.224
17	127	18.553	8.716	39.21
18	124	19.329	8.168	1.223
19	118	19.763	7.602	15.066
20	98	13.234	9.429	16.793

* Data from a K EDS map of a small area of M169.

Table DR1. Experiments summary

Sample	Annealing (min)	Deformation (min)	γ	Shear strain-rate (s^{-1})	Melta (vol. %)	OPXa (vol. %)	Ol grain size[a,b] (μm)	Grain boundaries density[b] (mm^{-1})
SM3	10	-	-	-	15.5	4.1	15.8	-
DD586	40	-	-	-	9.4	7.1	-	-
DD587	1000	-	-	-	2.5	15.2	-	-
M162	10	116	0.3	$4.9x10^{-5}$	5.3	10.4	10.3	358
M165	10	30	0.7	$3.78x10^{-4}$	1.6	12.9	11.1	478
M174	10	28	1.2	$7.08x10^{-4}$	1.3	13.8	10.7	409
M169	10	122	1.9	$2.57x10^{-4}$	1.8	14.1	10.1	415
M217	10	991	1	$1.7x10^{-5}$	1.6	9.9	15.5	304
M219	10	354	2	$9.6x10^{-5}$	1.2	11.3	14	354

[a] Measured after experiments

[b] Calculated from EBSD map data